

Standoff detection of biological aerosols by means of UV-laser induced fluorescence – results from Umeå trial 2006

Øystein Farsund and Gunnar Rustad

Forsvarets forskningsinstitutt/Norwegian Defence Research Establishment (FFI)

23 October 2008

FFI-rapport 2008/01990

100102

P: ISBN 978-82-464-1652-6

E: ISBN 978-82-464-1653-3

Keywords

Lidar

Fluorescens

Laser – anvendelse i biologi

Laser – anvendelse i overvåkning

Fjerndeteksjon

Ultrafiolett spektroskopi

Approved by

Hans Christian Gran

Project manager

Bjørn A. Johnsen

Director of Research

Jan Ivar Botnan

Director

English summary

The objective of standoff detection is to enable early warning in case of a biological warfare agent attack. FFI has built a demonstrator employing ultraviolet laser induced fluorescence of biological aerosols. The field campaign at FOI's premises in Umeå was an initial test of the instrument concept rather than a characterization of instrument sensitivity, probability of detection, false alarm rate and response time. Different biological warfare agent simulants were released in open air, and measured at 200-450 m standoff distance. The results substantiate the potential of discriminating and estimating concentration levels of various biological agents by means of their fluorescence emission spectra. Experiences and results from the campaign point to several possible instrument and test setup improvements.

Sammendrag

Målet med avstandsdeteksjon er å muliggjøre tidlig varsling i tilfelle angrep med biologiske stridsmidler spredt i form av aerosoler. FFI's demonstrator er basert på en teknikk hvor ultrafiolett laserlys induserer fluorescens i biologiske aerosoler. Fluorescensspekteret detekteres deretter av instrumentet. Feltkampanjen ved Totalforsvarets forskningsinstitut (FOI) i Umeå var en innledende test av instrumentkonseptet fremfor en karakterisering av instrumentparametre som følsomhet, deteksjonssannsynlighet, falsk-alarm-rate og reaksjonstid. Ulike simulanter for biologiske stridsmidler ble spredt i friluft og målt på 200-450 m avstand. Resultatene underbygger instrumentkonseptets potensial for å skjelne mellom og anslå konsentrasjonsnivå av forskjellige biologiske agens ved hjelp av deres fluorescensspektra. Erfaringer og resultater fra kampanjen peker på flere mulige forbedringer av instrument og testoppsett.

Contents

1	Introduction	7
2	Principle of measurement	7
2.1	Ultraviolet laser induced fluorescence	7
2.2	Fluorescence of biological molecules	8
3	FFI biolidar demonstrator	9
3.1	Instrument description	9
3.2	Instrument functionality	11
3.3	Calibration and characterization prior to Umeå trials	11
4	Trial description	12
4.1	Umeå test site	12
4.2	Test program	15
5	Results	16
5.1	Ambient conditions	16
5.2	Photo multiplier tube (PMT)	17
5.3	Fluorescence spectroscopy	18
5.3.1	Alignment check and spectral calibration	18
5.3.2	Setting the ICCD camera parameters	19
5.3.3	Measured BWA simulant spectra	21
5.4	APS reference measurement results	26
6	Conclusion	28
6.1	Discussion	28
6.2	Potential instrument improvements	29
	References	30
	Appendix A Release and data overview	31
A.1	Tuesday 28.11.2006	31
A.2	Wednesday 29.11.2006	32
A.3	Thursday 30.11.2006	34

1 Introduction

A prototype instrument for standoff detection of biological aerosols has been built within the frames of the FFI project 100102 "ARBC forsvar". The objective of standoff detection is to enable early warning in case of a biological warfare agent (BWA) attack, in order to bring preventive measures into action before contamination. One way of detecting biological aerosols at a distance, without contaminating the instrument, is based on ultraviolet laser induced fluorescence, which is the measurement principle of the instrument described herein. A UV laser pulse is fired at the biological agent, in which certain biological molecules are excited and reemit light at lower frequencies which is measured by the instrument. The aerosols also scatter light at the laser frequency. This elastic back-scattering is used to measure the distance from the instrument to the cloud of aerosols, as well as the depth of the cloud (Light Detection And Ranging, or *lidar*). Other research groups in the US, UK and Canada have developed the same type of standoff detection systems. FOI, Sweden, is planning to start a similar activity in 2008.

This report recapitulates the fundamental physical processes that form the base for the measurement principle. Moreover, the instrument is described. Most importantly, the results from field trials in Umeå (Sweden) on BWA simulants are presented and analyzed. Finally, lessons learned are summarized in the context of further work. The measurements betoken the instrument concept as a means for standoff detection of biological agents, as well as suggesting the concept may enable agent discrimination.

2 Principle of measurement

2.1 Ultraviolet laser induced fluorescence

The ultra violet laser induced fluorescence (UVLIF) technique is described in the following. A collimated UV laser pulse is emitted toward the bioaerosol cloud. Part of the light is scattered backwards without loss of energy (elastic scattering), while part of it is absorbed by biological molecules which subsequently emit light at lower frequencies than the excitation (laser) frequency (inelastic scattering, or fluorescence). A small amount of the scattered light is collected by the telescope and spectrally separated such that the elastically scattered light impinges a fast detector (photomultiplier tube, PMT), whereas the lower frequency light (fluorescence signal) is directed into a spectrograph and detected by a gated camera. The PMT measures the time of flight for the laser pulse, measuring the distance to and depth of the cloud of interest. These parameters are used to control the camera gating, in order to collect light from the range of interest. The signal from the bioaerosols is weak compared to the background in daylight conditions. As a consequence, the background should frequently be acquired and subtracted from the measurements.

The instrument needs optical visibility in the open line of sight throughout the operating range. In low visibility conditions such as fog or heavy precipitation other techniques should be employed,

if at all BWA releases are likely under such conditions. Naturally occurring biomolecules, *e.g.* pollen and fungi dispersed in the air, or plants, represent a challenge. In general, a ground based instrument can easier deal with fluorescing backgrounds such as plants, as the line of sight is parallel to the ground. An airborne instrument, however, will constantly face this challenge as it is looking toward the ground, usually covered by vegetation. Airborne measurements are additionally complicated because a potential BWA cloud will most likely be close to the ground. Moreover, a potential cloud of BWA will most probably spread in the horizontal direction favouring a horizontal-looking ground-based lidar.

2.2 Fluorescence of biological molecules

Fluorescence is a special case of luminescence – the emission of light not solely related to the temperature of the luminous object. In the process of fluorescence, absorption of incident radiation leads to an electronic transition within the molecule. As the molecule relaxes to its original state, a photon is emitted either directly (resonant fluorescence), or decays via vibrational transitions, interstate transfer, or lose vibrational energy through molecular collisions, before emitting a photon. The decay time of fluorescence is typically in the range from nanoseconds to milliseconds [1].

In this context two molecules are of particular interest; nicotinamide adenine dinucleotide (NADH) and tryptophan. NADH is important in cell respiration, therefore present in living bacteria. Tryptophan is a standard amino acid, hence a constituent also in virus. Tryptophan absorption peaks at 280 nm, and tryptophan fluorescence peaks around 350 nm. Their absorption and fluorescence spectra are shown in Figure 2.1 and Figure 2.2. Details on the interaction between light and biological matter is described in [2].

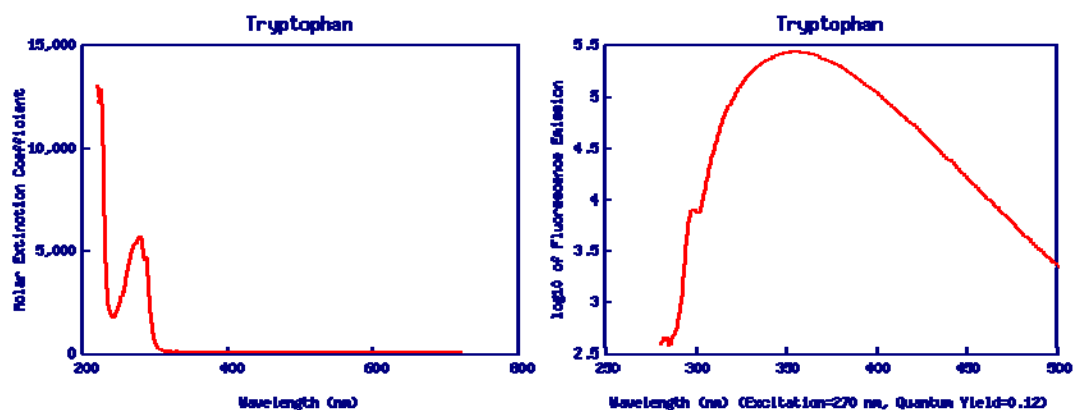


Figure 2.1: Fluorescence absorption (left) and emission (right) spectra for tryptophan [3]

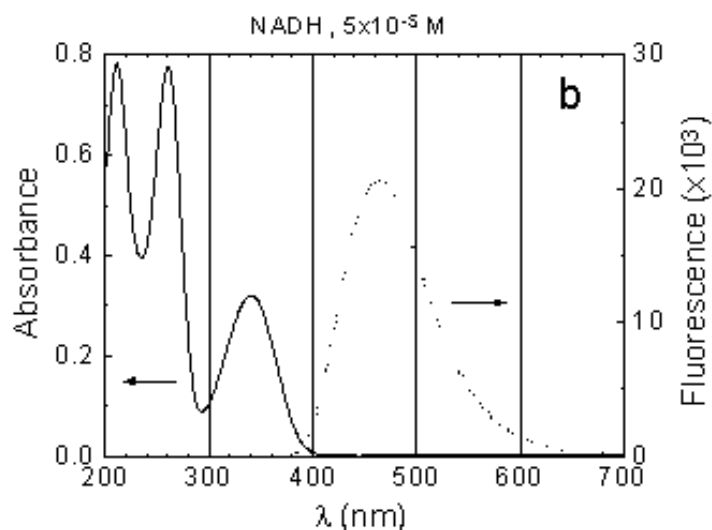


Figure 2.2: Picosecond absorption spectroscopy of a 5×10^{-5} M aqueous NADH solution [4]

3 FFI biolidar demonstrator

The instrument is thoroughly described in [5]. A short description is included below.

3.1 Instrument description

The demonstrator has been built using commercially available components. Key components are the laser and ICCD camera. The components have been mounted on a 750 mm x 1000 mm optical table. The main components are listed in Table 3.1 and the optical layout is shown in Figure 3.1. The breadboard is depicted in Figure 3.2.

Table 3.1: Some key components used in FFI's biolidar demonstrator

Component	Supplier	Model
Gated, intensified CCD camera	Andor	DH720_18mm
NdYAG laser with subsequent frequency conversion	Quantel	Brilliant b
Newtonian celestial telescope	Oriel	
Photo multiplier tube	Hamamatsu	

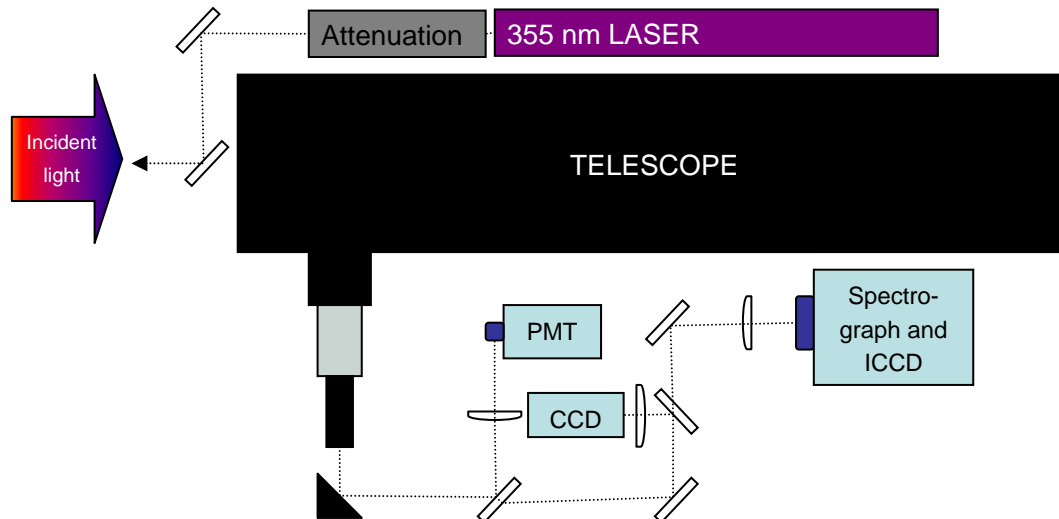


Figure 3.1: Schematic of biolidar

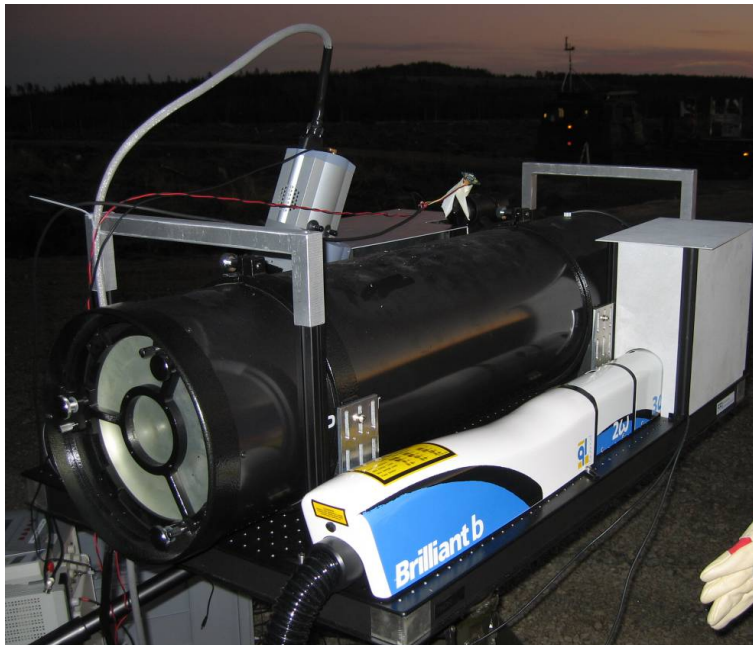


Figure 3.2: Breadboard with telescope (black cylinder), laser optical head (Brilliant b) and ICCD (grey box with cable)

The alignment of the laser and telescope is crucial. In order for the telescope field of view to overlap the laser beam at all relevant distances, the two optical axes should overlap. Moreover, the laser power has to be adjustable to compensate for distance to object as well as object characteristics (nature of fluorescence and particle density). The laser is placed next to the telescope, and the laser beam is aligned with the field of view by two adjustable mirrors, of which the final is placed on the optical axis of the telescope. Laser power reduction is carried out by means of a rotatable half-wave plate and a dielectric mirror which dumps one polarization of the beam onto a high power detector, enabling continuous monitoring of laser power. The optical table was mounted on a tripod with manually controllable tilt and rotation.

3.2 Instrument functionality

A brief description of the instrument functionality is as follows. A 5 ns long pulse at 1064 nm wavelength is emitted by the laser, subsequently converted to a UV pulse by nonlinear optical crystals. Appropriate pulse power is ensured by rotating the polarization relative to the dielectric mirror, and dumping the reflected part of the beam into the laser power meter. The residual 355 nm laser pulse is directed onto and along the optical axis of the telescope, and illuminates the field of view of the optical detection system. The field of view is determined by the position of the spectrograph slit in the telescope field of view. Center of the slit is accurately aligned with the center of the telescope focus. The optical system has 0.3 milliradian field of view in the across slit dimension, *i e* 30 cm at one kilometer distance. The UV laser pulse incident on a fluorescent object is partly scattered and partly absorbed, which leads to fluorescent emission. The scattered light represents our signal; however it is emitted in all directions and mixed with ambient (sun) light, which under certain conditions significantly reduces the signal to noise ratio. Thus only a small portion of the signal is collected by the telescope, dependent on the solid angle covered by the telescope and scattering properties of the target. The signal beam is collimated, in order for the optical detection to be aligned regardless of the object (thus focal) distance. The elastically scattered signal (at the laser frequency) is detached by means of a dichroic mirror, and focused onto the photo multiplier tube (PMT). The residual light is focused onto the spectrograph slit, grating and subsequently onto the ICCD detector.

The short pulse enables distance measurement to scattering objects (time of flight). This information is used to control the gating of the ICCD. A fast detector located close to the exit pupil of the laser detects the emission of the laser pulse, and triggers the oscilloscope measurement of the PMT signal. The time scale of the PMT signal can thus be converted to distance, hence recognizing areas of high elastic scattering. Similarly, the ICCD camera delay generator is triggered by the laser pulse emanation. The delay and gating width are adjusted according to the range of interest, in order to suppress background and signal inside the field of view, however temporally outside the gating window. The ICCD camera can be gated down to a 100 ns window, equivalent to 15 m, which is the maximum spatial resolution in the along the line of sight direction of the instrument. The PMT resolution is restricted by the PMT amplifier bandwidth (250 MHz) to approximately one meter.

3.3 Calibration and characterization prior to Umeå trials

The equipment was field tested for functionality and calibration purposes. Diesel combustion engine exhaust gas and flue gas from an oil heat central were used as targets. The instrument spectral response was also measured by looking towards the sky (Rayleigh scattered sun light) and comparing the result to a spectroradiometer [6]. The spectral response (quantum efficiency) of the ICCD camera is known. The instrument spectral response curve is shown in Figure 3.3.

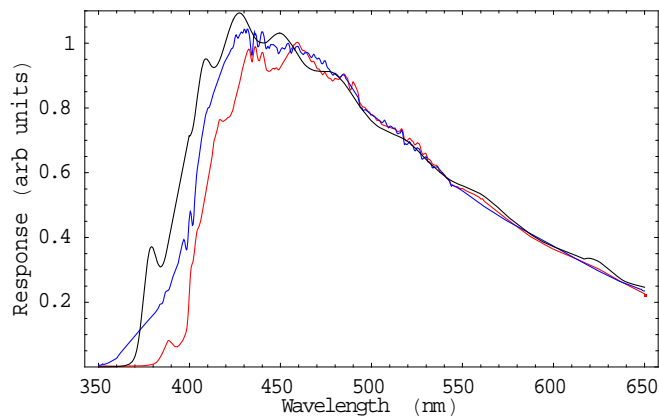


Figure 3.3: Theoretical spectral response of the biolidar (black) based on quantum efficiencies of ICCD camera and grating and laser mirror spectral response. Measured spectral response of the instrument: 1) including laser mirror spectral response (red) and 2) excluding laser mirror spectral response (blue). The discrepancy between theoretical and measured responses at UV wavelengths is affiliated to the spectral transmission of the optical components (refractive lenses, telescope and mirrors)

4 Trial description

4.1 Umeå test site

Totalforsvarets forskningsinstitut (FOI Swedish Defence Research Agency) has a proving ground for release of BWA simulants in Umeå. The field was constructed for point measurements; consequently standoff detection is possible at maximum 400 m distance from the release. FOI has planned to extend the site with a standoff detection course. The facility is the nearest of its kind to FFI (still approximately 1000 km away).

The proving ground is located in the woods, where a circular area with diameter exceeding 200 meter has been deforested. The center of the circle has a concrete slab with room for sensors as well as cabling from the control and observation barracks. FOI had several point sensors at this location. Roads at 100 and 200 meters radii have been worked up see Figure 4.1 and Figure 4.2



Figure 4.1: Aerial view of the Umeå proving ground (left). Instruments located at the center of the test site (right)



Figure 4.2: “Base camp” with personnel- and instrument barracks. The FFI biolidar and accessories were located under the blue tent

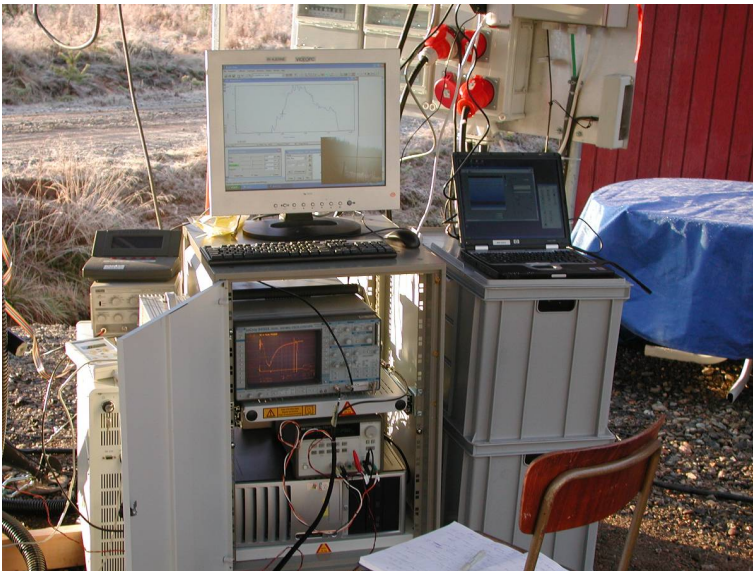


Figure 4.3: Operators “desk” during the field trial. The desktop PC controlled the ICCD, whereas the laptop controlled the PMT electronics



Figure 4.4: Field testing in the evening with no background (sun) light

A vehicle equipped with an aerosol generator is placed in position for the wind to bring the release to the center of the field. Personnel barracks and equipment containers are placed some 250 meters north of the field center. The barracks are pressurized and the inlet air is filtered in order to avoid contamination inside. Moreover, an on site 220 VAC generator supplies electric power. FFI chose to stay outside during the releases in order to be able to adjust all parameters not remotely controllable (such as pointing the telescope, optics alignment and laser power adjustment) see Figure 4.3 and Figure 4.4. Following this decision, we had to wear gas masks during release (Figure 4.5). However, the BWA simulants used do not represent any health risk (and it turned out that a simple dust protection mask would suffice). Walkie-talkies provided for communication. Dependent on meteorological data, the aerosol generator was located from 100 – 400 meters from the biolidar, thus, we were able to measure simulants at maximally 400 meters distance.



Figure 4.5: Operators staying outside during the releases had to wear gas masks

4.2 Test program

The field trial was directed by and for FOI, whereas FFI was allowed to participate. The test program was carried out in the period 28-30 November 2006. Three biological agents were released: Ovalbumin (OA), *bacillus thuringiensis* (BT) and *bacillus globigii* (BG). Some of the simulants were prepared wet (water solution) and sprayed, but most were released in dry condition (as powder). Some release data are given in Table 4.1.

Table 4.1: Test program for the November 2006 field trial in Umeå

Date	Approx time	Release No	Agent	Remark
28.11.2006		1	BT dry	High quantity release
		2	BT	Low quantity release
		3	OA	Twilight
		4	BT	Dark/ no ambient light
29.11.2006	11:10	1	5-10 g wet BT	Rain, fog, 1 km visibility
	11:25		300 g dry BT	
	13:30	2	50 g dry BG	
	13:45	3	1.3 l wet BT	
	14:25	4		
	15:20	5	Dry BT, dry OA	
	15:45		Dry OA	
30.11.2006	09:00	1	OA	Partly sunny, approx 0°C
		2	OA then BT	
		3	OA	
		4	BT then OA	
	11:15	5	BT then OA	

5 Results

The aim of the field trial was to demonstrate the operating principle and pick up valuable experience in further development of the instrument. The proving ground facility did not allow for sufficiently accurate reference measurements within the volume measured by the biolidar. Therefore characterizing instrument parameters such as sensitivity and accuracy was out of scope of this campaign.

The instrument achieved successful measurements the first day. It was misaligned the second day, probably as a consequence of cleansing the laser mirrors (which were covered by ice in the morning due to the cold night). The misalignment was discovered and fixed in the afternoon, after which appropriate measurement results were again obtained. Valuable fluorescence and elastic backscatter measurements were recorded the final day as well. The aim of the campaign was achieved.

5.1 Ambient conditions

During the measurement campaign, the temperature varied between $-5\text{ }^{\circ}\text{C}$ and $+5\text{ }^{\circ}\text{C}$. Illumination and humidity varied a great deal as the weather changed between sunny, overcast, fog and rain, see Figure 5.1. We also acquired data at dusk and in darkness (the sun sets early in November in northern parts of Sweden). The ambient light conditions are of major importance to the instrument sensitivity as ambient light forms the most significant contribution to the background noise level.



Figure 5.1: Examples of varying background light photographed from the instrument site. Simulants were released in light conditions varying from complete darkness to backlight from a setting sun almost in the instrument field of view. Measurements were also carried out in low visibility conditions such as fog and rain, with surprisingly high fluorescence signal

The background light was measured prior to the release, and this background level was subtracted from the measurement throughout the release, in order to extract the fluorescence signal. Thus background light level variations at minute scale cluttered the fluorescence signal.

5.2 Photo multiplier tube (PMT)

The PMT detects the elastically scattered laser light with a time resolution corresponding to approximately one meter. The PMT signal is used to find an aerosol cloud, furthermore the distance to it. The distance measurement is used to set the gating of the ICCD camera correctly. The PMT functionality was tested successfully. A typical scope trace of a PMT measurement is shown in

Figure 5.2.

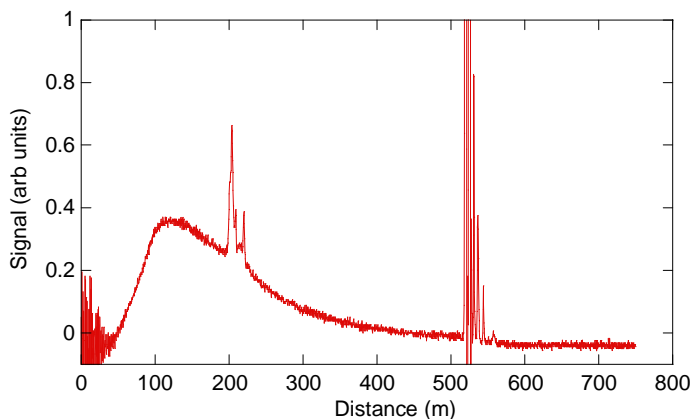


Figure 5.2: Typical oscilloscope trace from photo multiplier tube (PMT)

The envelope of the trace results from atmospheric particle backscatter. In an ideal instrument, the signal would be proportional to the inverse square of the distance to the particles ($1/R^2$). However, the low signal from 0 -100 m is a consequence of defocusing light scattered in this range. The telescope was focused to approximately 250 m. The released aerosol cloud was seen at approximately 200 m. The backscatter from the vegetation (trees) at 500 m saturated the PMT amplifier. In this situation, the ICCD camera gating for fluorescence measurement should start before 200 m and stop before the light scattered at 500 m reaches the detector. The ICCD gating was set to integrate the signal between 70 m and 450 m throughout the field test. In order to view the history of the PMT trace, a Labview program read and displayed the data as shown in Figure 5.3.

The PMT signal was of great use in finding and tracking the released particles. It was helpful to follow the cloud movement such that the release equipment could be located correctly for the aerosols to reach FOI's sensors located at the center of the proving ground. This was particularly valuable under difficult wind conditions.

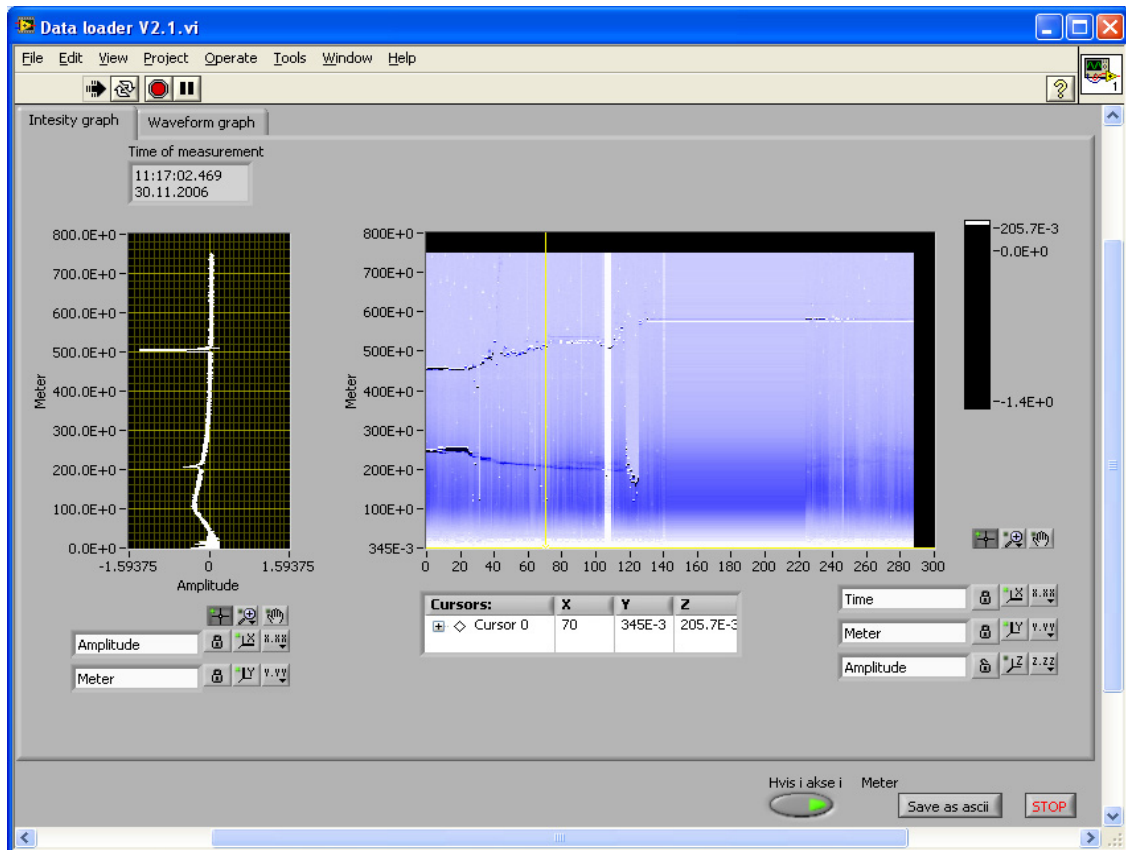


Figure 5.3: Screen dump of Labview program display. The code reads the instant PMT scope trace (left) and displays historic data by means of a color coded rainfall diagram (right)

5.3 Fluorescence spectroscopy

5.3.1 Alignment check and spectral calibration

In order to ensure alignment between laser and camera field of view, it is useful to point the instrument to the sky and integrate the signal from a long path. This way, Raman scattering by atmospheric constituents are measured, see Figure 5.4. Moreover, the Raman stokes shift is known as is the laser wavelength, thus absolute spectral calibration may be performed.

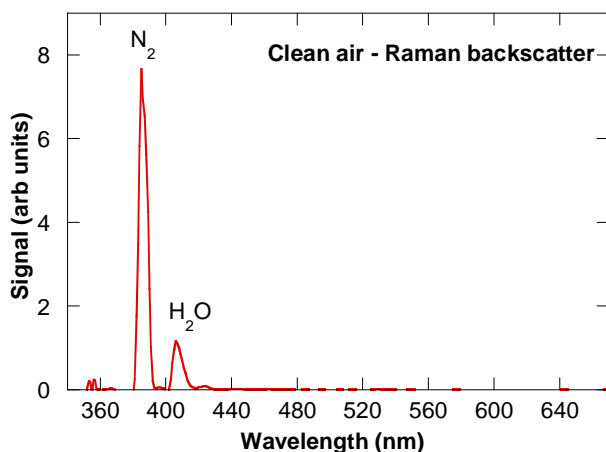


Figure 5.4: Raman backscatter acquired in clean air (neglectable amounts of fluorescent particles in the instrument line of sight). The Raman backscatter signal was used to confirm alignment of laser and camera field of view, as well as absolute wavelength calibration

The typical situation during a release is shown in Figure 5.5. The top photo shows the biolidar pointing towards the release equipment, which can dimly be perceived close to the woods on the other side of the proving ground (approximately 400 m away). The screen dump at the bottom: The cloud of released agent can be seen by the web camera looking through the alignment monocular on top of the telescope (Figure 5.6). The Andor IStar software (ICCD camera readout) shows the measured fluorescence spectrum, in this case with a strong signal as a consequence of the high BWA simulant concentration in the measurement path.

5.3.2 Setting the ICCD camera parameters

Several parameters for the ICCD camera have to be set. First of all, the timing has to be correct. That is, the camera should be gated when the fluorescent light of interest reaches the detector. A detector located by the laser exit pupil functions as trigger. The trigger starts timing a controlled delay which is generated by the camera electronics. The camera gating start (“delay”) and end (start + “pulse width”) are adjusted in software. Moreover, the ICCD gain has to be set (also in software) based on signal- and noise levels. Other camera features include pixel binning, background subtraction, summing of subsequent exposures, running average, and integrate on chip. All these parameters are set in order to optimize signal to noise ratio. Basically, the instrument was set to full vertical binning (no spatial resolution within the field of view), 7 pixels horizontal binning (accommodated to grating spectral resolution) and constant gating range.

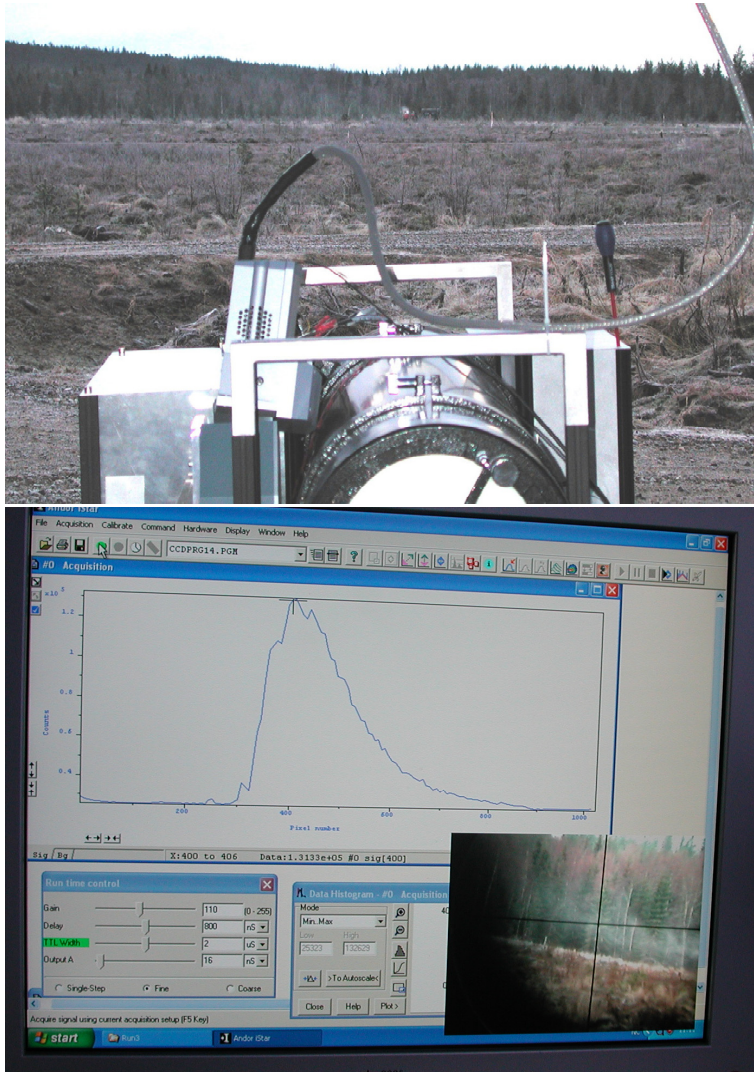


Figure 5.5: Typical situation during release: operator's view during release (top) and screen dump during the release (bottom). See text for detailed explanation

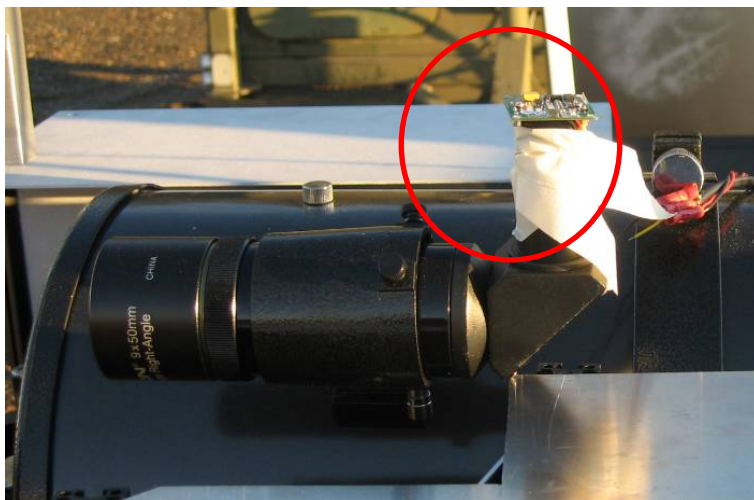


Figure 5.6: Camera looking through the telescope alignment monocular

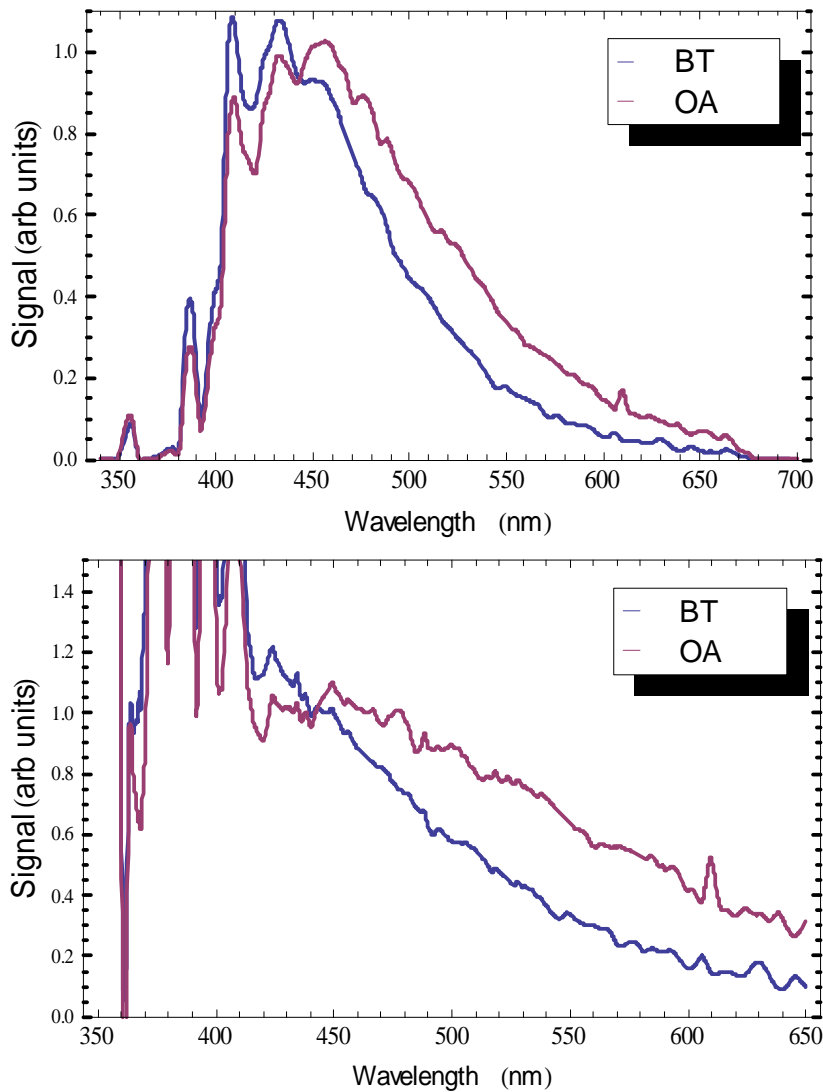


Figure 5.7: Measured spectra during releases of BT and OA, measured signal (top), responsivity-corrected data (bottom). The signals have been scaled

5.3.3 Measured BWA simulant spectra

An overview of the data is given in Appendix A. Typical biological agent spectra are shown in Figure 5.7. During release, the biolidar was aimed at the aerosol cloud. Once a significant signal was found, we tried to follow the cloud by maximizing signal as function of pointing direction. A time series during release of OA is given in Figure 5.8.

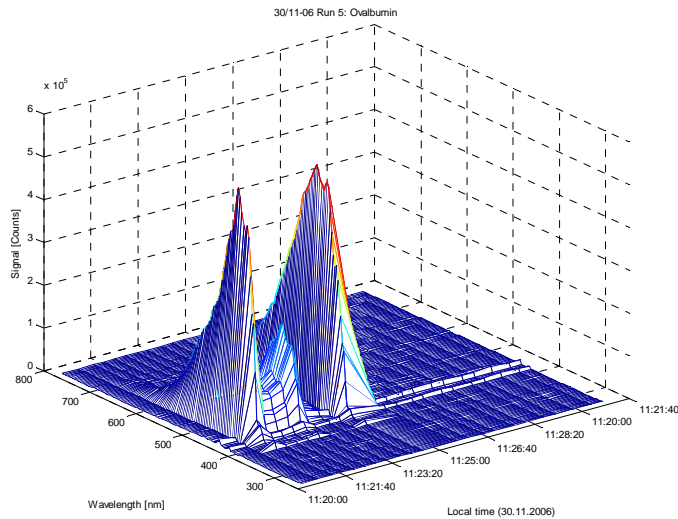


Figure 5.8: Time series of fluorescence spectral measurement during the release of OA. Two evident hits are seen in addition to Raman-scattering, which is measured throughout the time series

Selecting a spectrum with strong and another with neglectable OA signal, the spectral features of OA and Raman scattering are shown in Figure 5.9. Following the same procedure, BT spectral features are shown in Figure 5.10.

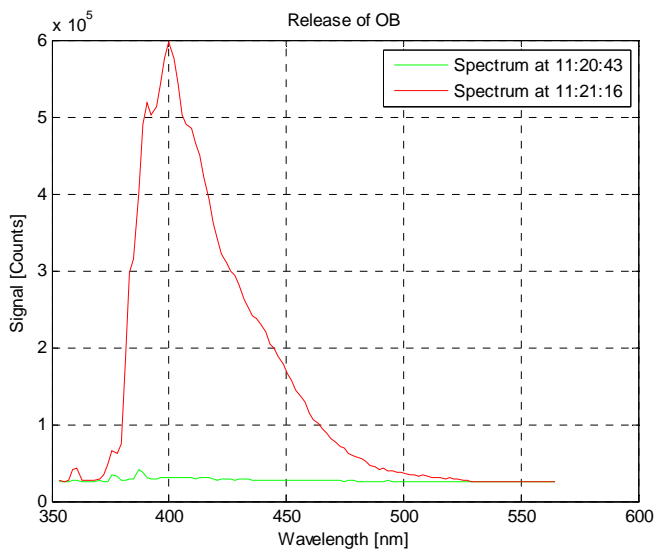


Figure 5.9: Fluorescence spectrum of ovalbumin (11:21) and Raman-scattering (11:20) measured during Run 5, 30.11.2006

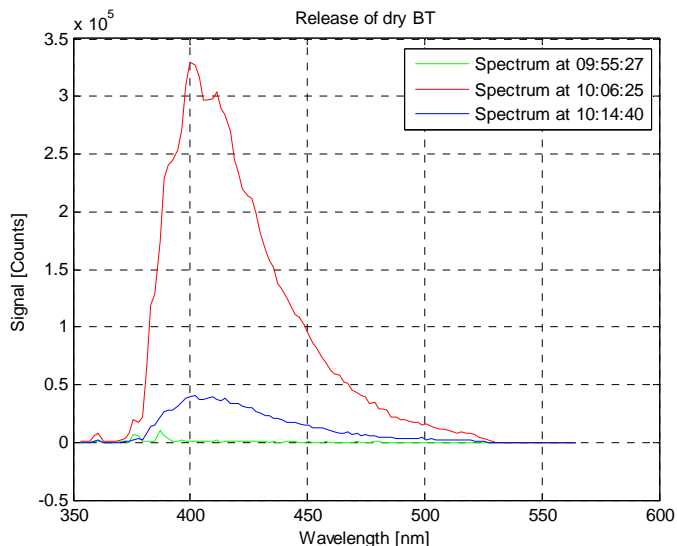


Figure 5.10: Fluorescence spectra measured during the release of BT (Run 2, 30.11.2006)

Unfortunately, the instrument suffered from poor alignment during the only BG release. All measured BG fluorescence spectra are therefore dominated by noise. Only very weak Raman scattering was observed immediately prior to and after release. Keeping this in mind, the best obtained spectra are included in Figure 5.11.

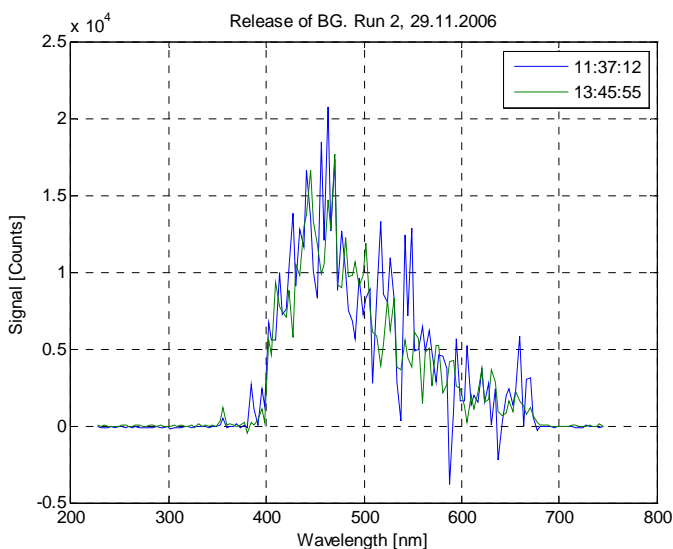


Figure 5.11: Fluorescence spectra measured during the release of BG (Run 2, 29.11.2006). The spectra are noisy owing to laser misalignment, however included because of BG's importance as a BWA simulant

During releases of BT and OA, spectra at different concentration levels were measured. In order to compare spectral features at varying concentrations, data were scaled. First, Raman scattered data (measurement with insignificant biological agent level under the same conditions and camera parameters) were subtracted. Subsequently, each spectrum was normalized with respect to its Euclidian norm. The results for BT and OA are presented in Figure 5.12 and Figure 5.13 respectively.

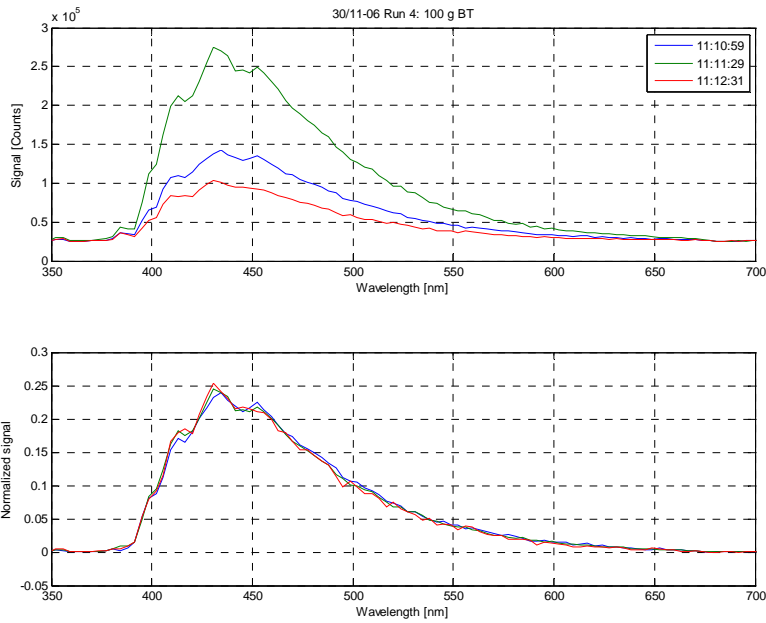


Figure 5.12: Four different concentration levels during the same BT release (Run 4, 30.11).
 Measured data (top) and scaled data (bottom): Measured Raman-scattering has been subtracted, followed by normalizing

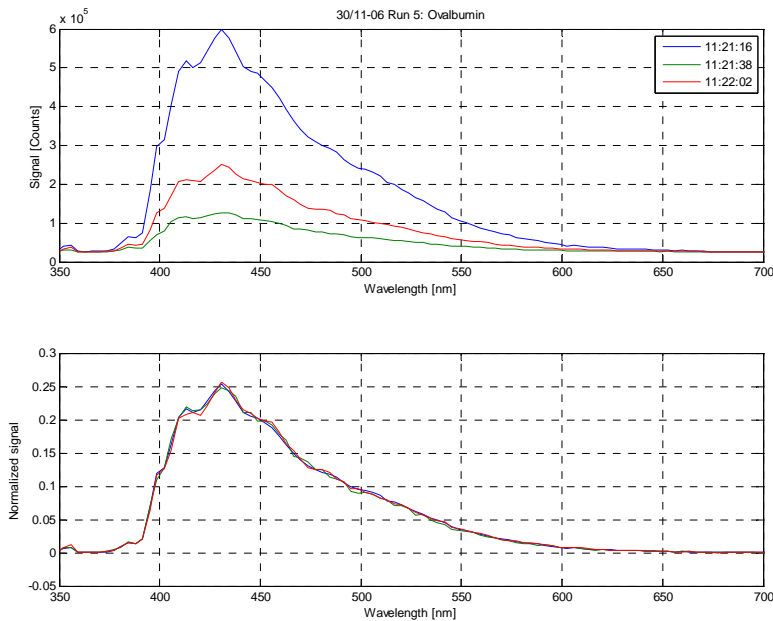


Figure 5.13: Three different concentration levels during the same OA release (Run 5, 30.11).
 Measured data (top) and scaled data (bottom): Measured Raman-scattering has been subtracted, followed by normalizing

The features of the fluorescence spectra appear constant with varying BWA simulant concentrations. It seems tenable to assume linear response as function of concentration. The best, still noisy BG spectrum has been normalized (without subtracting a Raman spectrum) and included in Figure 5.14 for comparison.

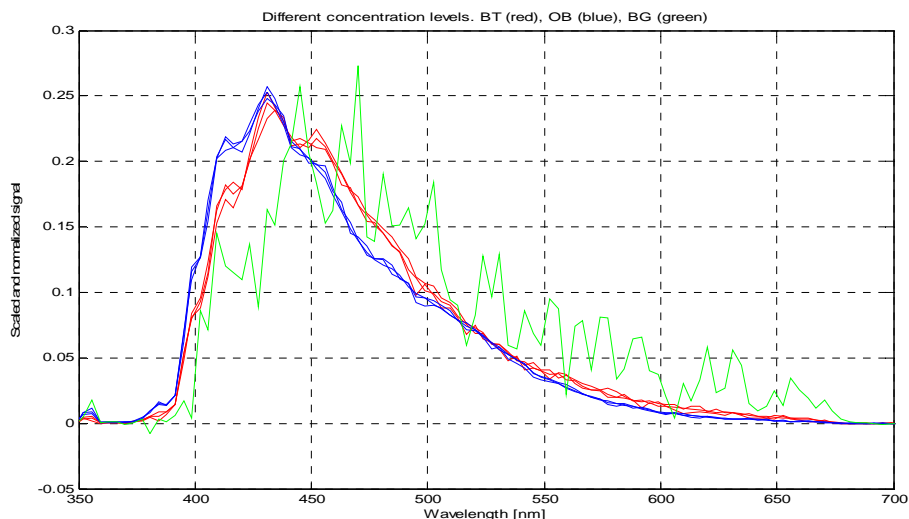


Figure 5.14: Scaled and normalized signals for different concentration levels of BT (red) and OA (blue). The only BG spectrum suffered from poor alignment between laser and ICCD field of view, however included for comparison with the other agents. The result suggests that the technique has the potential to separate agents by means of spectral features of the fluorescence

Our measurements point to the possibility of quantifying and discriminating agents appearing in a large dynamic range of concentrations, based on signal level and features of the fluorescence spectrum. Temporally and spatially overlapping release of different agents has not yet been tested.

Challenging situations emerge when fluorescent targets such as plants, pollen and exhaust (or two different simulants) come into the measured path. Solid state target signals are typically high compared to aerosol signals. Different plants have different fluorescence spectra. Thus several reference spectra have to be included in a future library in order to reduce false alarms from other biological material. A spectrum acquired as the laser was accidentally pointed to the ground (vegetation) is shown in Figure 5.15.

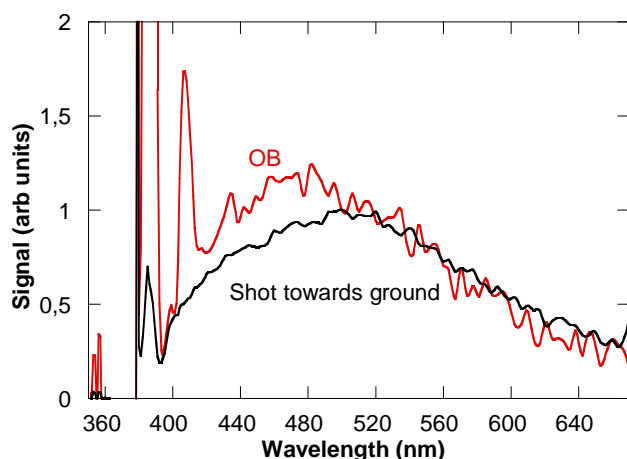


Figure 5.15: Fluorescence spectra of ovalbumin (OA) compared to a laser shot towards ground within the gating range

Another challenge is rapidly varying background illumination as mentioned above. The graphs in Figure 5.16 compare background drift with a spectrum of a biological agent.

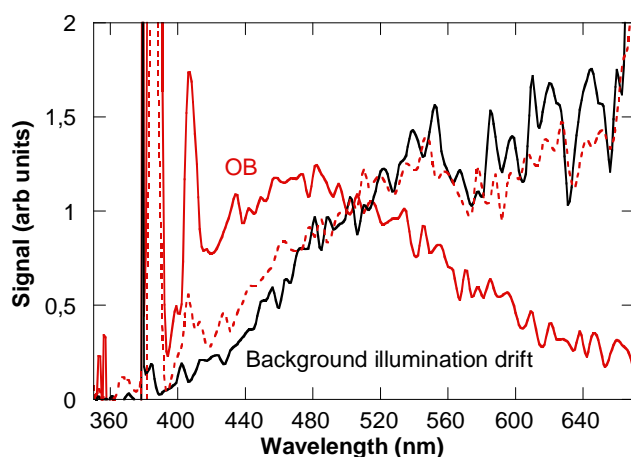


Figure 5.16: Scaled signals of OA measurement during stable background illumination (solid red), and during variation of background illumination: OA (dashed red), and without biological agent (solid black)

The measurement results are promising in the context of detecting potential biological agents at least at several hundred meters distance. They even point to capability of discriminating different biological substances by means of the measured fluorescence spectra.

5.4 APS reference measurement results

FOI had an aerodynamic particle sizer (APS) at the center of the proving ground. An APS collects ambient air, whose aerosol particles are accelerated by a sheath air flow and timed using two laser beams and photo multiplier tubes. The measured speed with which the particle travels depends on its aerodynamic diameter and mass. With sufficient calibration, the aerodynamic diameter and flow of particles are measured. Size distribution and concentration of particles can thus be

estimated [7]. The aerodynamic particle sizer used during the releases categorizes the aerosol diameters in 50 intervals from 0 – 20 μm . Background aerosols are generally small (less than one micron), whereas the released biological agent aerosols are typically in the 1 – 10 μm interval. The APS time series for all aerodynamic diameters measured 30.11.2006 is shown in Figure 5.17.

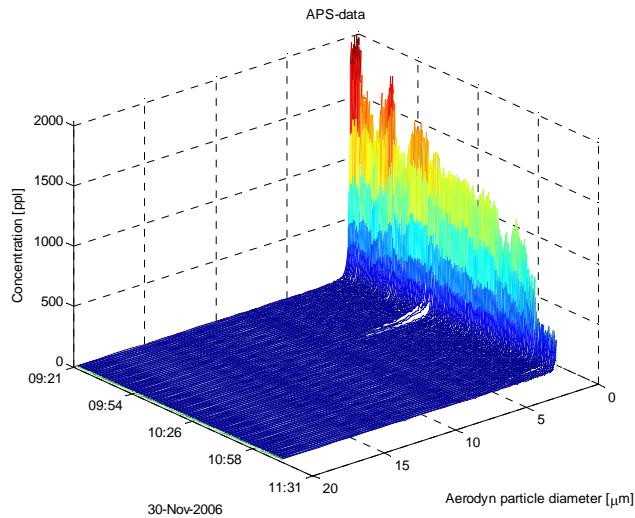


Figure 5.17: APS measurements. Flow of aerosols as function of their aerodynamic diameter and time. The background contains mostly small particles, whereas releases are in the 1-10 μm diameter range. The releases were significant, however not easily recognized in the plot

The releases do not stand out clearly; however there seems to be a few occurrences with significant non-background levels. The low signal is not surprising, as the agents are released in relative small quanta (approximately 100 g), then carried by the wind (hence diluted) some hundred meters before reaching the APS. Selected aerodynamic diameter intervals can be plotted separately in order elucidate the releases, however, this requires knowledge of which diameter range to search. Diameter intervals between one and ten micron have been plotted in Figure 5.18.

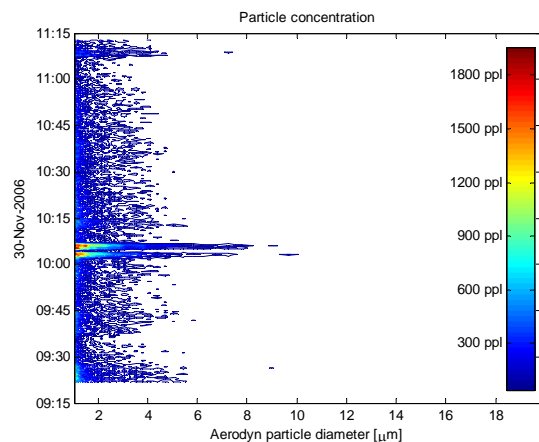


Figure 5.18: Contour plot of APS measurements from 1 – 10 μm aerodynamic diameter

A more general approach would be to plot the mean (or median as the background distribution is somewhat skew) of aerodynamic diameter, see Figure 5.19.

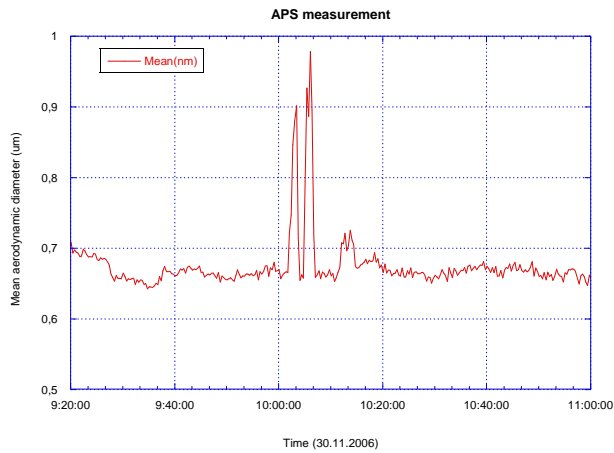


Figure 5.19: Mean aerodynamic diameter measured by APS 30.11.2006 indicates three hits from the release of aerosols between 10:00 and 10:20

The release hitting the APS at 10:07 is compared to the biolidar measurement. The measured average wind speed is approximately 2 m/s. The release took place some 200-400 m from center of the field, indicating that the start of the release took place 2-3 minutes before hitting the APS. The UVLIF measurements during this release are shown in Figure 5.20.

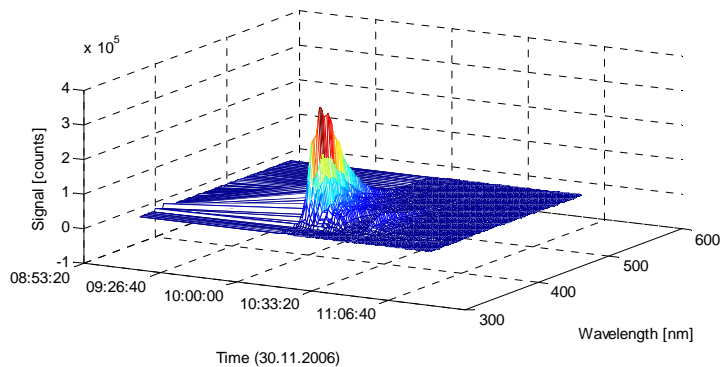


Figure 5.20: Time series of measured fluorescence 30.11.2006 around 10:00. The result correlates well with the simultaneous APS measurement. The lidar was pointed towards the released biological agent, and not above the center of the field

The APS measurements acquired in open air at the center of the field were not adequate for specifying instrument parameters such as sensitivity and response time. However, they substantiate a high probability of detection employing the biolidar.

6 Conclusion

6.1 Discussion

The Umeå field campaign was an initial test of the FFI biolidar instrument concept. The purpose of the campaign was to demonstrate the ultraviolet laser induced fluorescence technique, rather

than characterizing the instrument. The agents were released in open air. The biolidar was pointed in the direction which gave maximum signal, whereas an air particle sizer measured the aerosol concentration at the center of the proving ground. Thus there was no real reference to compare results with. Moreover, the instrument collected data without signal analysis capability. Therefore, important parameters such as sensitivity, probability of detection, false alarm rate and response time were out of scope of this field test. The fluorescence spectra presented herein are typical rather than exhaustive. OA and BT spectra were acquired under several conditions. BG however, was only released simultaneously with instrument alignment problems, thus the precision of the BG results is low.

Nevertheless, the acquired results fortify the potential of the UV LIF technique in standoff biological aerosol detection. The measurements, all carried out at 2-400 m distance, substantiate the potential of discriminating various biological agents by means of their fluorescence emission spectrum. In order to measure important instrument parameters, accurate reference measurements with respect to the amount of agent in the instrument “volume of sight” should be aimed at in future campaigns.

6.2 Potential instrument improvements

The field testing addressed weaknesses and possible instrument improvements as listed below.

- Protection of breadboard against rain and wind using a windshield or telescope visor to eliminate splash on laser mirror
- Simultaneous, synchronized recording of
 - video from telescope ocular
 - PMT results
 - UV LIF spectra
 - (audio - comments)
- Frequent background measurements
 - A field instrument can not depend on ambient light conditions. Therefore it is crucial to implement sufficiently frequent background acquisitions. Preferential is an alternating automatic recording of background and signal. Furthermore, subtract background from signal on the fly, and sum 1-100 subsequent acquisitions
- Simplified power supply and cabling to optical table
- Avoid PMT saturation by elastic scattering within the nearest 200 m
 - PMT gating or fast onset
- Synchronization with other groups' instruments
 - GPS time stamp or synchronization of PCs
- Mechanical fastening of ocular camera
- Monitor able to show both PC and video (or digital camera employing USB-interface)
- Smaller oscilloscope
 - time resolution of 0.2 $\mu\text{s}/\text{div}$ is sufficient
- All programs run from the same PC

The above mentioned measures are affordable at moderate efforts. Several have been implemented (by 1.3.2008).

References

- [1] R M Measures. *Laser remote sensing - fundamentals and applications*. Krieger publishing company, Malabar, Florida, 1992.
- [2] M Sletmoen. *Vekselvirkning mellom lys og biologisk materiale*. FFI-notat 2008-00828 (In Norwegian), FFI, Kjeller, 2008. www.ffi.no
- [3] A T Timperman, K E Oldenburg, and J V Sweedler. Native fluorescence detection and spectral differentiation of peptides containing tryptophan and tyrosine in capillary electrophoresis. *Anal. Chem.*, 67: 3421-3426, 1995.
- [4] S Pakalnis, V Sitas, H Schneckenburger, and R Rotomskis. Picosecond absorption spectroscopy of biologically active pigments NADH, FMN and fluorescence marker Rhodamine-123. In: *The Third Internet Photochemistry and Photobiology Conference*, J Photochem. Photobiol. B: Biology, (www.photobiology.com/photobiology2000, 2000),
- [5] G Rustad and Ø Farsund. *Standoff detection of biological aerosols by UV-laser induced fluorescence*. FFI-rapport 2008/02025, FFI, Kjeller, 2008. www.ffi.no
- [6] *FieldSpecPro Full Range User's Guide, rev C*. Analytical Spectral Devices Inc, Boulder, CO, 2002. www.asdi.com
- [7] W C Hinds. *Aerosol technology: properties, behavior, and measurement of airborne particles*. 2nd ed., Wiley, New York, 1999.

Appendix A Release and data overview

A.1 Tuesday 28.11.2006

Run1		Run2		Run3		Run4	
0	Luft, Raman	1	Raman	1	Raman	1	Raman
1	Fluor, Raman	2	Raman	2	Støy	2	Raman
2	Fluor, Raman	3	Fluor	3	Raman	3	Raman
3	Fluor, Raman	4	Svak fluor, Raman	4	Støy	4	Raman
4	Fluor, Raman	5	Raman	5	Støy	5	Raman
5	Svak fluor, Raman	6	Raman	6	Svak fluor	6	Bakken?
6	Svak fluor, Raman	7	Fluor	7	Støy	7	Bakken, svak?
7	Svak fluor, Raman	8	Raman	8	Svak fluor	8	FLuor/Bakken
8	Svak fluor, Raman	9	Raman	9	Svak fluor	9	Bakken
9	Svak fluor, Raman	10	Raman	10	Raman, Støy	10	Bakken, svak?
10	Svak fluor, Raman	11	Raman	11	Raman, Støy	11	Bakken
11	Raman	12	Raman	12	Raman, Støy	12	Støy
12	Raman	13	Raman	13	Raman, Støy	13	Støy
13	Svak fluor, Raman	14	Raman	14	Raman, Støy	14	Støy
14	Fluor, Raman	15	Raman	15	Støy	15	Bakken
15	Fluor, Raman	16	Fluor	16	Sollys?	16	Bakken
16	Raman	17	Fluor	17	Svak fluor	17	Støy
17	Raman	18	Fluor	18	Svak fluor	18	Svak fluor?
18	Sollys?	19	Fluor	19	Raman		
19	Støy	20	Sollys?	20	Raman		
20	Støy	21	Fluor	21	Raman		
21	Støy	22	Fluor, støy	22	Raman		
22	Støy	23	Fluor, støy	23	Raman		
23	Støy	24	Støy, sollys?	24	Raman		
		25	Fluor	25	Raman		
		26	Fluor, sollys	26	Raman, Støy		
		27	Sollys?				
		28	Sollys?				
		29	Støy				
		30	Støy				
		31	Støy				
		32	Støy				

A.2 Wednesday 29.11.2006

Run 4		Run 5 (reopplinjert laser)	
1	Støy	1	Fluor, raman
2	Fluor, bakken?	2	Fluor, raman
3	Fluor, bakken?	3	støy
4	Støy	4	støy
5	Støy	5	støy
6	Støy	6	støy
7	Støy	7	støy
8	Støy	8	støy
9	Støy	9	støy
10	Fluor, bakken?	10	støy
11	Støy	11	støy
12	Støy	12	støy
13	Støy	13	støy
14	Støy	14	støy
15	Støy	15	støy
16	Støy	16	støy
17	Støy	17	støy
18	Støy	18	støy
19	Støy	19	0-fil
20	Støy	20	0-fil
21	Støy	21	test?
22	Støy	22	test?
23	Støy	23	test?
24	Støy	24	test?
25	Støy	25	test?
26	Støy	26	test?
		27	test?
		28	test?
		29	test?
		30	test?
		31	test?
		32	test?
		33	test?
		34	test?
		35	test?
		36	test?
		37	test?
		38	test?
		39	test?
		40	test?
		41	test?
		42	test?
		43	test?
		44	test?
		45	test?
		46	test?
		47	test?
		48	462 nm??
		49	633 nm

50	Raman
51	Raman
52	Raman
53	Fluor, raman
54	Fluor, raman
55	Fluor, raman
56	Fluor, raman
57	Fluor, raman
58	Raman
59	Fluor, raman Sterk Fluor,
60	raman
61	Raman
62	Raman
63	Fluor, raman
64	Raman
65	Raman
66	Fluor, raman
67	Raman
68	Raman
69	Raman
70	Fluor, raman
71	Raman
72	Raman
73	Raman
74	svak fluorescens
75	Raman
76	Raman
77	svak fluorescens
78	Raman
79	Raman
80	Raman
81	Fluor, raman
82	Fluor, raman Sterk Fluor,
83	raman Sterk Fluor,
84	raman
85	Fluor, raman Sterk Fluor,
86	raman
87	svak fluorescens
88	Fluor, raman
89	Fluor, raman
90	svak fluorescens
91	Raman
92	Raman
93	Fluor, raman
94	Fluor, raman
95	Fluor, raman
96	Raman
97	Raman
98	Raman Sterk Fluor,
99	raman
100	Raman

A.3 Thursday 30.11.2006

Run 1	Run2	Run 3	Run 4	Run 5
1 Fluor, sollys?	17 Raman	1 Bakgrunn	38 Fluor	1 Svak fluor
2 Fluor, sollys?	18 Fluor	2 Bakgrunn	39 Fluor	2 Svak fluor
3 Fluor, sollys?	19 Fluor	3 Bakgrunn	40 Fluor	3 Fluor
4 Fluor, sollys?	20 Fluor	4 Bakgrunn	41 Fluor	4 Fluor
5 Fluor, sollys?	21 Fluor	5 Bakgrunn	42 Fluor	5 Fluor
6 støy	22 Fluor	6 Bakgrunn	43 Fluor	6 Fluor
7 støy	23 Fluor	7 Bakgrunn	44 Fluor	7 Fluor
8 støy	24 Fluor	8 Bakgrunn	45 Fluor	8 Brederer fluor?
9 Fluor, sollys?	25 Fluor	9 Raman	46 Fluor	9 Brederer fluor?
		raman +		
10 Fluor, sollys?	26 Fluor	10 støy	47 Svakere fluor	10 Svak fluor
		raman +		
11 Raman, støy	27 Fluor	11 støy	48 Fluor	11 Fluor
		raman +		
12 Raman, støy	28 Fluor	12 støy	49 Fluor	12 Fluor
		raman +		
13 Raman, støy	29 Fluor	13 støy	50 Fluor	13 Svak fluor
		raman +		
14 Raman, støy	30 Fluor	14 støy	51 Fluor	14 Svak fluor
15 Fluor, raman	31 Fluor	15 svak fluor	52 Fluor	15 Svak fluor
16 Raman	32 Fluor	16 fluor	53 Fluor	16 Svak fluor
		fluor +		
	33 Fluor	17 bakgrunn?	54 Svakere fluor	17 Svak fluor
		fluor +		
	34 Fluor	18 bakgrunn?	55 Svakere fluor	18 Svak fluor
		fluor +		
	35 Fluor	19 bakgrunn?	56 Svakere fluor	19 Svak fluor
	36 svak fluor	20 Bakgrunn	57 Svakere fluor	20 Svak fluor
	37 Fluor	21 Bakgrunn	58 Fluor	21 Svak fluor
	38 Fluor	22 Bakgrunn	59 Fluor	22 Svak fluor
		fluor +		
	39 Støy fluor	23 bakgrunn?	60 Fluor	23 Svak fluor
		fluor +		
	40 Støy fluor	24 bakgrunn?	61 Svakere fluor	
		fluor +		
	41 Støy fluor	25 bakgrunn?	62 Svakere fluor	
		fluor +		
	42 Støy fluor	26 bakgrunn?	63 Svakere fluor	
		fluor +		
	43 Støy fluor	27 bakgrunn?	64 Svakere fluor	
		fluor +		
	44 Støy fluor	28 bakgrunn?	65 Fluor	
		fluor +		
	45 Støy fluor	29 bakgrunn?	66 Svakere fluor	
		fluor +		
	46 Fluor	30 bakgrunn?	67 Fluor	
		fluor +		
	47 Fluor	31 bakgrunn?	68 Fluor	
		fluor +		
	48 Fluor	32 bakgrunn?		
		fluor +		
	49 Fluor	33 bakgrunn?		
		fluor +		
	50 Fluor	34 bakgrunn?		
	51 Fluor	35 fluor +		

			bakgrunn?
			fluor +
52	Fluor	36	bakgrunn?
			fluor +
53	Fluor	37	bakgrunn?
54	Fluor		
55	Støy fluor		
56	Støy fluor		
57	Støy fluor		
58	Støy fluor		
59	Støy fluor		
60	Støy fluor		
61	Støy fluor		
62	Støy fluor		
63	Støy fluor		
64	Støy fluor		
65	Støy fluor		
66	Støy fluor		
67	Støy fluor		
68	Støy fluor		
69	Støy fluor		
70	Støy fluor		
	bakgrunn,		
71	fluor		
	bakgrunn,		
72	fluor		
	bakgrunn,		
73	fluor		
	bakgrunn,		
74	fluor		
	bakgrunn,		
75	fluor		
	bakgrunn,		
76	fluor		
	bakgrunn,		
77	fluor		
78	støy		
79	støy		
80	støy		
81	støy		
	støy,		
82	bakgrunn?		
	støy,		
83	bakgrunn?		
	støy,		
84	bakgrunn?		